Identification of a dengue 2 virus envelope protein receptor in *Aedes aegypti* critical for viral midgut infection

Asher M. Kantor[a,1], Octavio A. C. Talyuli[a,1], William R. Reid[b], Patricia Hessab Alvarenga[a], Jasmine Booker[a], Jingyi Lin[b], Alexander W. E. Franz[b] (ID), and Carolina Barillas-Mury[a,2] (ID)

Affiliations are included on p. 8.

The establishment of a productive dengue virus (DENV) infection in the midgut epithelial cells of *Aedes aegypti* is critical for the viral transmission cycle. The hypothesis that DENV virions interact directly with specific mosquito midgut proteins was explored. We found that DENV serotype 2 (DENV2) pretreated with trypsin interacted with a single 31 kDa protein, identified as AAEL011180 by protein mass spectrometry. This putative receptor is a highly conserved protein and has orthologs in culicine and anopheline mosquitoes. We confirmed that impairing the expression of AAEL011180 in the midgut of *Ae. aegypti* females abolished the interaction with DENV2, and the virus also bound to immobilized recombinant purified receptor. Furthermore, recombinant DENV2 surface E glycoprotein bound to recombinant AAEL011180 with high affinity (38.2 nM) in binding kinetic analysis using surface plasmon resonance. The gene for this DENV2 E protein receptor (EPrRec) was disrupted, but since the gene is essential in *Ae. aegypti*, only heterozygote knockout (ΔEPrRec^{+/−}) females could be recovered. Further reducing EPrRec mRNA expression in the midgut of ΔEPrRec^{+/−} females by systemic dsRNA injection significantly reduced the prevalence of DENV2 midgut infection. EPrRec also interacts with heat shock protein 70 cognate 3 (Hsc70-3), and silencing Hsc70-3 expression in ΔEPrRec females also reduced the prevalence of DENV2 midgut infection.

dengue Virus | *aedes aegypti* | E protein Receptor | mosquito | midgut

Dengue is worldwide the most widespread viral infection transmitted by mosquitoes. Infection with any of the four serotypes of dengue virus (*Flaviviridae*; *Orthoflavivirus*; DENV1-4) has a broad clinical spectrum. Although a majority of DENV infections are asymptomatic, they often result in "break-bone fever," consisting of fever, severe headache, eye pain, as well as muscle and joint pain. However, the disease can be severe and progress to dengue hemorrhagic fever, which can be fatal (1, 2). There is no specific antiviral treatment for DENV, so therapies focus on symptom management, and patients with severe dengue disease require hospitalization. Recently, the WHO documented that DENV infections have been on the rise from about 500,000 cases in 2000 to over 9,000,000 cases in 2024 (3). Modeling suggests that 3.9 billion people are currently at risk of DENV infection, with the disease endemic in over 100 countries (4, 5).

DENV circulates between mosquito vectors and human hosts in urban horizontal transmission cycles. *Aedes aegypti* and *Ae. albopictus* are the principal DENV vectors. A mosquito becomes infected when a female takes a viremic blood meal from a human during probing/feeding. The midgut of *Ae. aegypti* is the primary tissue infected by DENV following ingestion of an infectious blood meal (6). The blood meal enters the midgut lumen of the mosquito and virions within the blood meal start to infect the midgut epithelial cells (7). Following replication in the midgut epithelium, the virus disseminates from the mosquito midgut to secondary tissues including the salivary glands. Once those are infected, the mosquito can persistently transmit the virus during probing on human hosts (8).

The four DENV serotypes have a positive-sense ssRNA genome, ~10,700 bp in size, encoding three structural proteins (C, prM/M, and E) and seven nonstructural proteins (NS1, NS2A, NS2B, NS3, NS4A, NS4B, and NS5) (9, 10). C surrounds the viral RNA genome (11), while prM/M and E glycoproteins are associated with the lipid bilayer of the enveloped virion (12). The crystal structure of the E protein showed that it has three distinct domains, with domain three containing an immunoglobulin-like structure with cellular binding motifs and epitopes that mediate cell surface receptor attachment (11, 13–15). Inside the midgut lumen, virus comes into direct contact with proteolytic enzymes secreted by the mosquito as the blood meal undergoes digestion. Previous studies showed that enzymatic modification of DENV virions by trypsin enhances their

Significance

The four serotypes of the dengue virus (DENV1-4) are the most medically relevant arboviruses and are transmitted by the mosquito *Aedes aegypti* in tropical regions of the world. Here, we identified an envelope (E) protein receptor (EPrRec) for DENV2 in the midgut of *Ae. aegypti*. Impairing the expression of EPrRec decreased the prevalence of DENV2 infection in mosquitoes. Additionally, we found that EPrRec interacts with Hsc-70-3 and showed that the interactions between EPrRec, the DENV2 E protein, and Hsc-70-3 occurred during the early stages of viral infection. These protein interactions were crucial for DENV2 to establish a productive midgut infection in *Ae. aegypti*. Targeting these interactions could be explored as a strategy to disrupt DENV2 transmission.

interaction with the midgut epithelium (16). Once DENV is internalized by an epithelial cell via receptor-mediated endocytosis, the viral E protein is responsible for membrane fusion and virion uncoating inside the mature endosome (17–19). Previously, interactions of DENV with several proteins present in mosquito cultured cells or mosquito tissues were reported, and it was proposed that they could mediate infection (20–25). However, these interactions have not been fully characterized in vivo to assess their role in DENV infection of *Ae. aegypti* mosquitoes.

The molecular interactions mediating the initial establishment of DENV infection in midgut epithelial cells are not well understood. Here, we identify a mosquito DENV2 E protein receptor ("EPrRec") that localizes to the submicrovillar region of midgut epithelial cells and interacts with the heat shock protein 70 cognate 3 (Hsc70-3). We demonstrate that reducing EPrRec or Hsc70-3 expression by dsRNA-mediated silencing in heterozygote knockout ("ΔEPrRec") females prevents the establishment of DENV2 midgut infection in *Ae. aegypti*.

Results

DENV2 Interacts with Specific Mosquito Midgut Proteins. The interactions between DENV2 and midgut epithelial cells were explored using a virus overlay protein binding assay (VOPBA) to establish whether DENV virions interact directly with specific mosquito midgut proteins. Midguts were dissected 48 h postfeeding of mosquitoes on blood serum. The insoluble pellet fraction of the midgut homogenate, which included cell membranes and cytoskeleton-associated proteins, was subjected to SDS/PAGE electrophoresis under denaturing/nonreducing conditions (samples were heated to 70° C after the addition of SDS loading buffer) and transferred to a nitrocellulose membrane, followed by protein denaturation and refolding. Multiple weak interactions with proteins of 31 kDa, 36 kDa, 47 kDa, and 53 kDa were observed when the membrane with the immobilized proteins was incubated with purified DENV2 (Fig. 1*A*). Because the virus is naturally exposed to digestive enzymes excreted into the midgut lumen during blood meal digestion, the effect of proteolytic cleavage of DENV2 virions on protein–protein interactions was explored by digesting virus particles in vitro with bovine trypsin, followed by trypsin inactivation with soybean trypsin inhibitor (STI) before incubation with the membrane-immobilized proteins. After proteolytic processing, DENV2 virions interacted strongly with a single 31 kDa protein (Fig. 1*A*). The identity of the protein(s) interacting with DENV2 was established by subjecting the midgut membrane fraction to two-dimensional (2D) gel electrophoresis. Proteins were transferred to a nitrocellulose membrane and probed with purified DENV2. A single spot of the expected molecular weight (31 kDA) was detected in the membrane (Fig. 1*B*) and the corresponding spot (S-1) as well as two other negative control spots (S-2 and S-3), were excised from the gel and subjected to mass spectrometry analysis (Fig. 1*B*, *SI Appendix*, Fig. S1 and Tables S1–S3). The *Ae. aegypti* protein encoded by AAEL011180 was the most abundant protein in the excised spot with 81 peptides (*SI Appendix*, Table S1). This putative midgut receptor is a highly conserved protein that has orthologs in culicine and anopheline mosquitoes. Indeed, it is

Fig. 1. Characterization of DENV2 interactions with specific proteins in *Ae. aegypti* midgut homogenates. (*A*) *Left* image: Coomassie-stained gel (*Left*) of cellular membrane and cytoskeletal midgut extract (MG ext) fraction. Next three images: Binding of DENV2 (DV), DENV2 pretreated with trypsin (DV-T), and a no bait control to membrane-immobilized midgut extracts in far-western blots. Midguts were collected at 48 h postfeeding of mosquitoes on human serum and the homogenate fraction was separated by SDS/PAGE. (*B*) *Left*: 2D Coomassie-stained gel of cellular membrane and cytoskeletal midgut extract fraction. *Right*: Binding of DENV2 to membrane-immobilized midgut extracts in a 2D far-western blot. The protein spot excised from the SDS-gel corresponding to the spot where DV-T bound to the membrane is indicated by the red box. (*C*) *Left*: RT-qPCR quantification of the putative receptor (Rec) mRNA transcripts in midguts following intrathoracic injection of mosquitoes with dsRNA derived from the putative receptor mRNA (dsRec) or a LacZ dsRNA (nontarget) control (dsLZ). Next three images: Coomassie-stained gel of cellular membrane and cytoskeletal midgut extract fraction following dsRec injection. Effect of dsRNA silencing on DV-T binding to midgut protein extracts in a far-western blot. The membrane was stripped and then reprobed with anti-actin-HRP antibodies in a western blot using actin as a sample loading control. (*D*) *Left*: Coomassie-stained SDS/PAGE gel showing purified recombinant Rec. Center: DV-T binds to immobilized recombinant Rec in a far-western blot and (*Right*) in the ELISA; *t* test, * *P < 0.05*. (*E*) Binding kinetics of different concentrations (500, 250, 125, 62.5, 31.5, 15.6, and 7.8 nM) of recombinant Rec protein to immobilized DENV2 E protein by surface plasmon resonance (K_d = 38 nM).

the ortholog of the P47 receptor, a midgut receptor in *Anopheles gambiae* that interacts with the *Plasmodium falciparum* surface protein Pfs47. Furthermore, this interaction allows the parasite to evade the mosquito immune system by inhibiting Caspase S2-mediated apoptosis (26). We confirmed that silencing expression of the putative receptor (Rec) by systemic injection of dsRNA almost completely abolished DENV2 binding to the immobilized midgut homogenate (Fig. 1*C*), confirming that the interaction of DENV2 is specific and mediated by Rec. Furthermore, DENV2 also bound to immobilized, recombinant (purified) Rec in the VOPBA and ELISA (Fig. 1*D*). The affinity of the interaction of recombinant DENV2 surface E glycoprotein with recombinant Rec was also determined with a binding kinetic analysis using surface plasmon resonance (Fig. 1*E*). Soluble recombinant protein encoded by AAEL011180 bound to immobilized DENV2 E glycoprotein with a Kd of 38.2 nM. Based on this high-affinity interaction, we are referring to this protein as the E protein Receptor (EPrRec).

Subcellular Localization of EPrRec. The subcellular localization of EPrRec in the mosquito midgut was established by immuno-fluorescence staining of midguts dissected 24 h postfeeding of mosquitoes on human serum using antibodies generated against the EPrRec ortholog in *An. gambiae*, as previously described (26). The *An. gambiae* antibodies were specific and recognized a single protein of the expected molecular weight (32 kDa) in *Ae. aegypti* midgut homogenates (*SI Appendix*, Fig. S2). EPrRec was expressed in all epithelial cells with a predominant localization at the apical side of the cell (Fig. 2*A*). A high-resolution confocal cross section of epithelial cells revealed that EPrRec antigen was localized directly below the microvilli and was found in high abundance at the cell-to-cell junctions within the apical side of the cell, toward the gut lumen (Fig. 2*B*), similar to what has been observed in *An. gambiae* (26). Interestingly, 4 d after DENV2 infection EPrRec antigen was still localized toward the apical half of the cell, but exhibited a broader distribution, and was no longer confined to the submicrovillar region (Fig. 2*C*), while DENV2 antigen was evenly distributed throughout the cell cytoplasm.

Effect of EPrRec Silencing on DENV2 Infection of *Ae. aegypti*. The high affinity of EPrRec to DENV2 E glycoprotein and its submicrovillar localization suggest that EPrRec may be involved in early stages of DENV2 midgut infection. To explore this hypothesis, we investigated the effect of reducing EPrRec expression on DENV2 infection in the mosquito via gene silencing by intrathoracic injection of a 472 bp dsRNA targeting *EPrRec*. In the treatment group of 45 mosquitoes, we observed an average reduction of *EPrRec* mRNA levels in the mosquito by 10-fold (90% reduction) at the time of DENV2 infection, 4 d postinjection (Fig. 3*A*). However, the transient nature of dsRNA-mediated silencing in the midgut (27), combined with natural high *EPrRec* mRNA expression levels (similar to the highly expressed housekeeping gene *RPS7*) only allowed partial silencing of the gene's expression as its average cycle threshold (CT) value in qRT-PCR assays was still relatively low, reaching a value of 23.9. (*SI Appendix*, Table S4). Observed effects of transient EPrRec mRNA silencing on DENV2 midgut infection at 7 d postinfectious blood meal were modest and variable. A 2.67-fold decrease in the median DENV2 titer per mosquito was observed in an initial experiment, while in a second replicate, there was a modest (4.5-fold) increase in median virus titers (*SI Appendix*, Fig. S3). When the data from the two independent biological replicates were combined, EPrRec silencing did not result in a significant difference regarding the prevalence or intensity of DENV2 infection in the mosquito midgut compared to *dsLacZ*-injected (nontarget) control mosquitoes (Fig. 3*A*). To
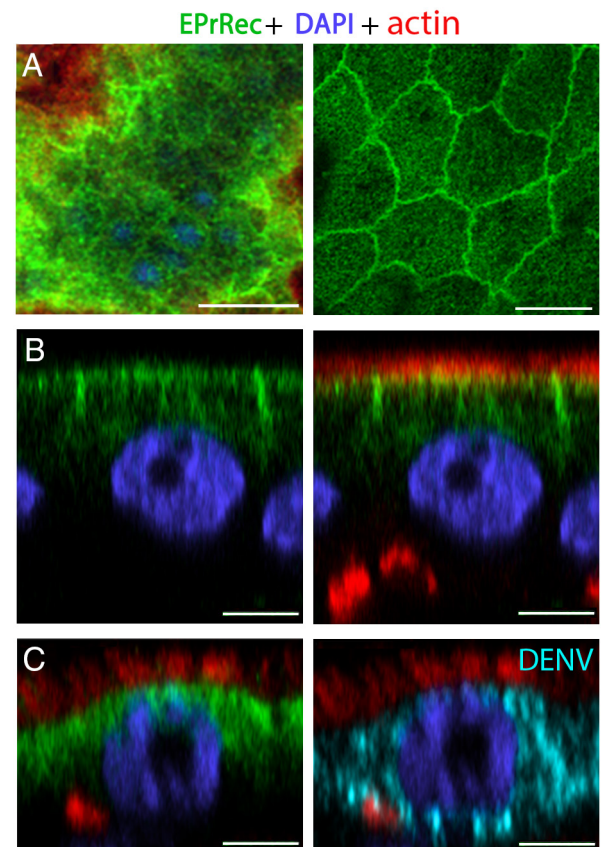

Fig. 2. Subcellular localization of EPrRec in midgut epithelial cells of *Ae. aegypti*. (*A*) EPrRec (green) localizes to the apical section of the midgut epithelium at 24 h postfeeding of mosquitoes on serum (*Left*) and in cell-to-cell junctions (*Right*). (*B*) Side view of epithelial cells with EPrRec (green) localized to the submicrovillar region just below actin-rich microvilli (red). (Scale bars, 10 μm.) (*C*) EPrRec (green) localizes to the apical cytoplasm region in DENV2 (light blue)-infected epithelial cells at 4 d postinfection of mosquitoes via an infectious blood meal. (Scale bars, 5 μm.)

establish whether a more profound and long-lasting reduction of EPrRec expression would affect DENV2 infection levels, we decided to use a transgenic approach to disrupt the EPrRec gene.

CRISPR/Cas9 Mediated Disruption of the EPrRec Gene in *Ae. aegypti*. The EPrRec gene was disrupted via eye marker containing transgene insertion using CRISPR/Cas9 gene editing. Following pretesting in a transient assay with *Ae. aegypti* embryos, an sgRNA (sgRNA 3, *SI Appendix*, Table S5) targeting the 5' end of exon 2 of AAEL011180 for cleavage at nucleotide position 80 of the coding sequence was selected for the disruption of the gene. The insertion (knock-in) transgene consisted of an eye tissue–specific mCherry expression cassette linked to left and right homology arms flanking the sgRNA target site (Fig. 3*B*).

For the targeted disruption of AAEL011180, a total of 1305 pre-blastoderm *Ae. aegypti* Liverpool strain (LVP) embryos were injected with the mix described in the Methods section and 153 of them (11.7%) survived. These developed into 59 female and 94 male G_0 founders. The G_0 individuals were outcrossed to WT LVP mosquitoes and the resulting G_1 offspring were screened for mCherry eye marker expression. mCherry-positive mosquitoes were outcrossed to WT LVP mosquitoes for one more generation to obtain a ΔEPrRec line. The transgene insertion was confirmed by PCR, choosing oligonucleotide primer pairs annealing to sequences surrounding the 5' and 3' junction regions of the transgene insertion site. Sanger-sequencing of the PCR products indicated that the transgene was inserted at the correct site for gene disruption of
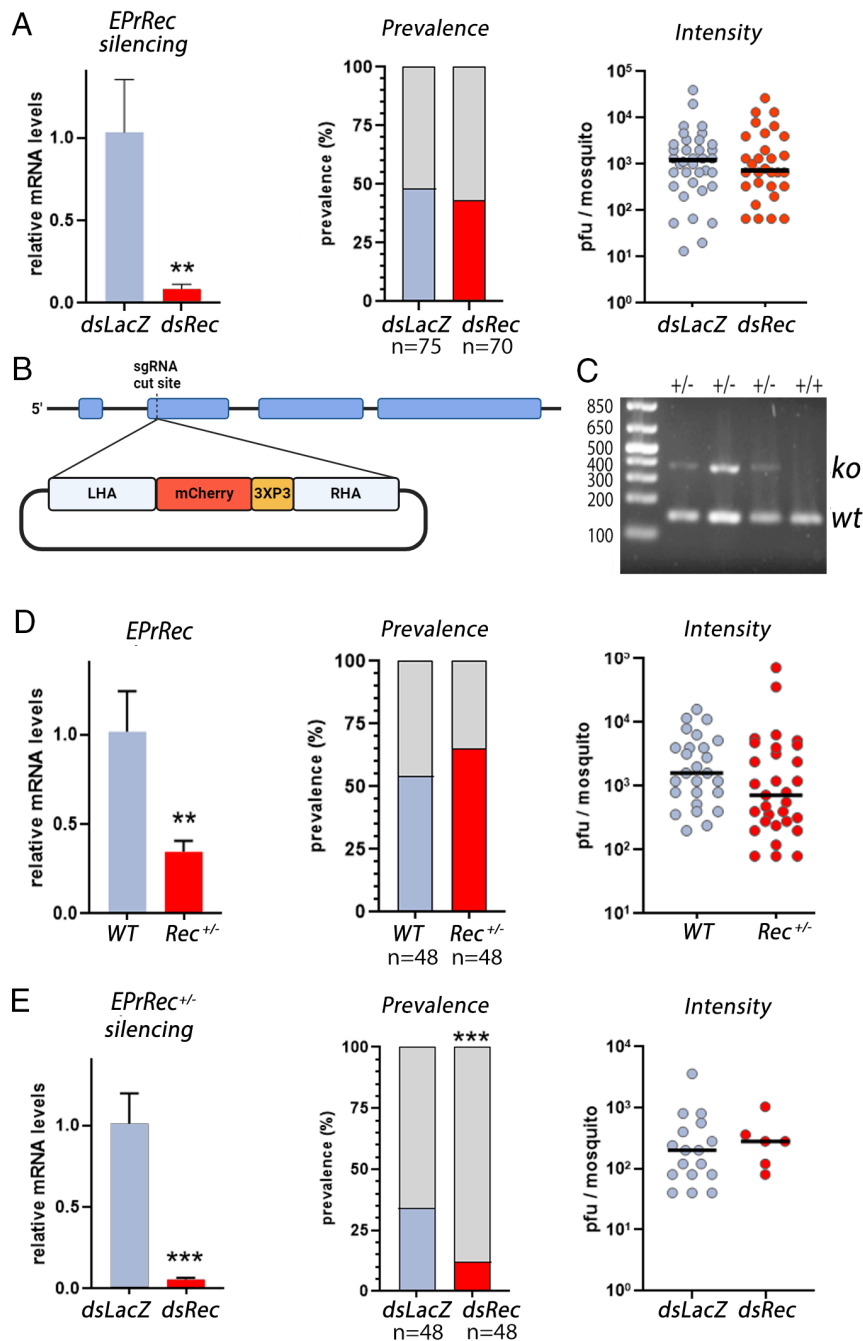
Fig. 3. Effect of EPrRec silencing on DENV2 infection of *Ae. aegypti*. (*A*) *Left*: RT-qPCR quantification of EPrRec mRNA in midguts 4 d post-intrathoracic injection of dsRNA targeting EPrRec (dsRec) or LacZ (dsLacZ; nontarget control), *t* test *P* < 0.01. Center: Effect of EPrRec silencing on DENV2 infection prevalence and (*Right*) on virus titers (intensity of infection) in midguts. Mosquitoes were offered a DENV2 containing artificial bloodmeal 4 d postinjection of dsRNA. Midguts were collected at 7 d postinfection with DENV2. Virus titers were determined by the plaque assay, and horizontal lines represent median DENV2 titers. (*B*) Schematic of the gene structure of AAEL011180 (pERec) and the design of the insertion construct to facilitate CRISPR/Cas9-mediated gene disruption. Using sgRNA #3, the genomic DNA would be cleaved at nucleotide position 80 of the coding sequence of AAEL011180 (located at the 5' end of the 2. exon). LHA: left homology arm; RHA: right homology arm; 3xP3: promoter to drive eye tissue–specific gene expression of the mCherry marker; SV40: transcription terminator. (*C*) Genotyping of individual female ΔEPrRec mosquitoes using a multiplex PCR assay. The 375 bp band signal is indicative of an allele harboring the insertion transgene that disrupts pERec (ko), while the 130 bp band signal is indicative of the wild-type (WT) allele. Hemizygous individual (+/−); WT individuals (+/+). (*D*) *Left*: RT-qPCR quantification of EPrRec mRNA transcripts in midguts of ΔEPrRec$^{+/−}$, and WT *Ae. aegypti*; *t* test, *P* < 0.01. Center: Infection prevalence and (*Right*) virus titers in individual midguts of ΔEPrRec$^{+/−}$, and WT *Ae. aegypti* at 5 d postinfection of mosquitoes with DENV2. Virus titers were determined by the plaque assay, and horizontal lines represent median DENV2 titers. (*E*) *Left*: RT-qPCR quantification of EPrRec mRNA transcripts in midguts of ΔEPrRec$^{+/−}$ mosquitoes following silencing via dsRNA injection targeting EPrRec (dsRec) or control LacZ (dsLacZ); *t* test, *P* < 0.001. Center: Infection prevalence and (*Right*) virus titers in individual midguts of ΔEPrRec$^{+/−}$ and WT *Ae. aegypti* at 5 d postinfection of mosquitoes with DENV2. Mosquitoes had been intrathoracically injected either with dsRec to silence EPrRec or with dsLacZ as a nontarget control. Fisher's exact test, *P* = 0.0003. Virus titers were determined by the plaque assay, and horizontal lines represent median DENV2 titers.

EPrRec. Finally, eye marker–positive G$_2$ mosquitoes were intercrossed over several generations followed by selection to generate homozygous individuals. A multiplex PCR genotyping assay that generated a PCR amplicon of 130 bp and 375 bp for the detection of WT and ΔEPrRec alleles, respectively, was established to screen for transgene-bearing females and identify homozygous individuals. (Fig. 3*C*). After genotyping several hundreds of individual adult mosquitoes, we were unable to detect a single homozygous transgenic individual. This led us to conclude that EPrRec is an essential gene and its biallelic loss of function is causing lethality. We then evaluated

EPrRec mRNA expression levels in hemizygous (ΔEPrRec$^{+/-}$) adult females and found that expression was reduced by 65% relative to WT mosquitoes (Fig. 3D). This rather expected reduction in EPrRec mRNA levels when just one of the two alleles was disrupted in ΔEPrRec$^{+/-}$ females, unfortunately, had no effect on prevalence or intensity of midgut infection in multiple DENV2 challenge experiments (Fig. 3D).

Regardless, EPrRec expression was further reduced by 94% on average (compared to the dsLacZ control) when applying dsRNA-mediated silencing of the target gene in ΔEPrRec$^{+/-}$ females (Fig. 3E). In these mosquitoes, the prevalence of DENV2 infection was significantly reduced from 35% to 12% (Fisher's exact test, $P = 0.0003$) (Fig. 3E). Strikingly, dsRec injected ΔEPrRec$^{+/-}$ females, when infected, generated similar DENV2 titers as the control, suggesting that EPrRec played an important role early in the establishment of DENV2 midgut infection but rather less so in viral replication inside the midgut epithelium or dissemination from the midgut to secondary tissues. These data demonstrate that a specific interaction between EPrRec and DENV2 virions is key for efficient midgut infection of the virus.

EPrRec Interacts with Heat Shock Protein Hsc70-3 in the Midgut of *Ae. aegypti*. To further investigate the role of EPrRec in DENV2 infection of *Ae. aegypti*, we sought to explore potential interactions of EPrRec with other candidate proteins. Recently, the *An. gambiae* ortholog of EPrRec was shown to interact with the molecular chaperone heat shock protein 70 cognate 3 (Hsc70-3). This interaction prevents the activation of caspase-mediated nitration in mosquito midgut epithelial cells invaded by *Plasmodium* ookinetes (28). We investigated whether *Ae. aegypti* Hsc70-3 also interacts with EPrRec by expressing recombinant Hsc70-3 in *Escherichia coli* and performing ELISAs, in which Hsc70-3 was immobilized on the ELISA plate and incubated with serial dilutions of EPrRec (Fig. 4A). The binding of EPrRec to Hsc70-3 was saturable with an estimated 50% of maximum binding at a soluble recombinant EPrRec concentration of 70.68 nM (Fig. 4B). The effect of transient silencing of Hsc70-3 on DENV2 infection of ΔEPrRec$^{+/-}$ females was evaluated. Intrathoracic injection of Hsc70-3 dsRNA reduced Hsc70-3 mRNA levels on average by 70% compared to the dsLacZ nontarget control (Fig. 4C), and significantly decreased the prevalence of DENV2 infection from 53% to 24% (Fisher's exact test, $P < 0.001$) in these mosquitoes. Hsc70-3 silencing had no effect on the intensity of infection in those females that became infected.

Discussion

In this study, we identified a DENV2 E protein receptor, EPrRec, and characterized some of its key interactions with the virus and other host factors in the midgut of *Ae. aegypti*. Previous studies identified proteins from *Ae. aegypti* or *Ae. albopictus* cell lines that interacted with DENV serotypes 1-4, such as prohibitin, enolase, and a tubulin-like cytosolic protein interacting with DENV2, a laminin-binding protein interacting with DENV3,4, and a HSP90-related protein as well as cadherin interacting with DENV2,4 (20, 23, 29). Other uncharacterized glycoproteins from midgut and salivary gland homogenates were also shown to interact with DENV serotypes 1-4 (22, 25, 30, 31). There are no orthologs of EPrRec in vertebrates or other insects besides mosquitoes. Furthermore, EPrRec has no homology to any of the putative receptor proteins previously reported. These studies suggest that DENV probably does not bind to a single receptor to infect mosquito cells but may interact with multiple proteins on the cell surface or in the cytosol. However, from these studies, it

remains unresolved, exactly which of these interactions are critical for DENV to successfully infect the mosquito midgut and to disseminate to other tissues including the salivary glands, and whether there are different DENV receptors in different cell types.

EPrRec was primarily localized to the submicrovillar region on the apical side of a midgut epithelial cell as well as in cell-to-cell junctions and not within the cell membrane, suggesting that EPrRec may not be a typical viral membrane receptor (Fig. 2 A and B). The subcellular localization of EPrRec suggests that DENV2 virions may interact with this protein during the early stages of viral entry into a midgut epithelial cell. We demonstrated that in vitro proteolytic processing of DENV2 with trypsin altered the interaction of the virus with midgut proteins, resulting in stronger and more specific binding to EPrRec. In vivo, this proteolytic processing may take place within the midgut lumen during blood meal digestion. Alternatively, EPrRec may interact with cytosolic proteases, such as a previously characterized epithelial serine protease (ESP), which localizes to the submicrovillar region in midguts of *An. gambiae* (32) and that has an ortholog in *Ae. aegypti*. ESP plays a key role in the infection of the *An. gambiae* midgut by *Plasmodium* parasites (32). The fact that multiple attempts to generate a homozygous ΔEPrRec line had failed in our hands, strongly suggests that the EPrRec gene has an essential developmental role. The high level of expression of this gene in mosquito midgut cells made it necessary to further transiently reduce its expression in ΔEPrRec$^{+/-}$ females before an effect on DENV2 infection prevalence could be observed.

EPrRec is the ortholog of the previously characterized P47Rec (26). Both genes have four exons and encode 290-amino-acid proteins containing four DM9 domains, which lack signal peptides or any transmembrane domains. The proteins share 83% identity and 91% homology at the amino acid level and their predicted structures as revealed by AlphaFold (https://alphafold.ebi.ac.uk/) are very similar (*SI Appendix*, Fig. S4). EPrREC also has clear orthologs in other culicine and anopheline mosquitoes (26). DM9 domain-containing proteins were first described in *Drosophila*, but there is no ortholog of EPrRec (33). In Pacific oysters (*Crassostrea gigas*), DM9 domain-containing proteins were recently shown to function as Pattern Recognition Receptors with the ability to bind a broad range of pathogen-associated molecular patterns (34). In *An. gambiae*, the interaction between *Plasmodium* Pfs47 and the mosquito P47Rec allows the parasite to disrupt a caspase-mediated apoptotic response that activates nitration in parasite-invaded midgut cells, a critical reaction for mosquitoes to mount an effective immune response against the parasite (26, 28). Lack of epithelial nitration allows the parasite to evade the mosquito complement-like system and to survive.

A screen of downstream effectors in *An. gambiae* identified Hsc70-3 as a key mosquito protein interacting with P47Rec (28). Furthermore, reducing the expression of Hsc70-3 activated caspase S2-dependent apoptosis in parasite-invaded midgut cells and reduced parasite survival (28), indicating that the interaction of P47Rec with Hsc70-3 was critical to inhibit a caspase-mediated apoptotic response. It is intriguing that the interaction of EPrRec with Hsc70-3 is also critical for DENV2 midgut infection as it has been reported that *Ae. aegypti* mosquitoes that are refractory to DENV2 control the viral infection through a caspase-mediated apoptotic response (35); and overexpression of Hsp70 in WEHI–S murine fibrosarcoma cells has an antiapoptotic effect by inhibiting late caspase-dependent events (36). Furthermore, a recent study showed that the *Ae. aegypti* ortholog of Hsc70-3 regulates DENV2 replication by interacting with the viral NS1 protein (37); here, we demonstrate another direct interaction of Hsc70-3 with EPrRec. This interaction, when disrupted, led to a decrease in DENV2
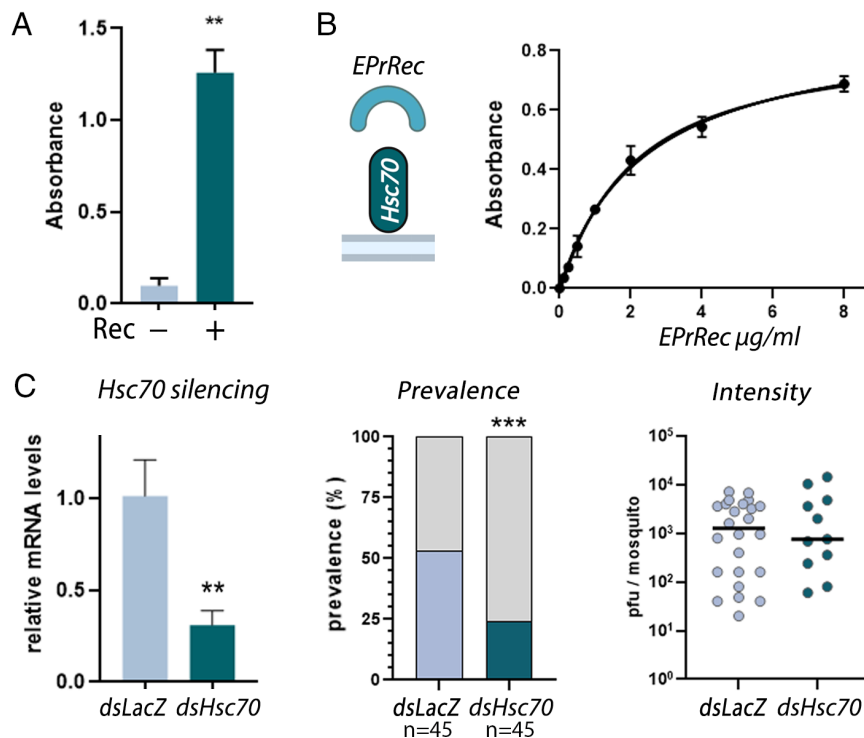
Fig. 4. EPrRec interacts with Hsc70 to establish DENV2 infection of midguts in *Ae. aegypti*. (*A*) Recombinant EPrRec binds to immobilized recombinant Hsc70 in the ELISA. *t* test, $P<0.01$. (*B*) *Left*: Schematic representation of recombinant EPrRec binding to immobilized recombinant Hsc70 in the ELISA. *Right*: Binding of increasing concentrations of recombinant EPrRec to immobilized recombinant Hsc70 in the ELISA. (*C*) *Left*: RT-qPCR quantification of Hsc70 mRNA in midguts of ΔEPrRec$^{+/-}$ females following intrathoracic injection of dsHsc70 RNA into ΔEPrRec$^{+/-}$ females to silence Hsc70 (dsHsc70) or LacZ dsRNA as a nontarget control (dsLacZ). *t* test, $P < 0.01$. Center: Effect of Hsc70 silencing on DENV2 infection prevalence and (*Right*) virus titers (intensity of infection) in individual midguts of ΔEPrRec$^{+/-}$ females. Fisher's exact test, $P < 0.001$. Midguts were assayed at 5 d postinfection of mosquitoes with DENV2 via infectious blood meals. Virus titers were determined by the plaque assay, and horizontal lines represent median DENV2 titers.

infection prevalence, but not in the viral intensity of infection. This suggests that the interaction of EPrRec with Hsc70-3 is important during an early step in the DENV2 infection process of midgut epithelial cells. Once midgut cells have become productively infected, reducing EPrRec or Hsc70-3 expression had no effect on viral dissemination from the organ. Taken together, our findings suggest that EPrRec and P47Rec are members of a broad-spectrum protein family, which are targeted by different pathogens to suppress caspase-mediated apoptosis through interaction with Hsc70-3. Blocking apoptosis during the early steps of infection may be critical for DENV2 to establish a productive infection of the midgut. These observations beg the question of whether EPrRec and Hsc70-3 are also critical for the establishment of other arboviral midgut infections besides DENV2 including other *Ae. aegypti* transmitted ortho-flaviviruses and alphaviruses (i.e., DENV1, 3, 4, Zika, yellow fever, chikungunya viruses). If these interactions are conserved, they could represent a target to develop a broad strategy to prevent disease transmission of multiple arboviruses by *Ae. aegypti* mosquitoes.

Materials and Methods

Mosquitoes and DENV2 Infection. *Ae. aegypti* (strain: Liverpool; LVP) and ΔEPrRec$^{+/-}$ mosquitoes were reared at 27° C and 80% humidity under a 12-h light/dark cycle. They were maintained under laboratory conditions and fed 10% sucrose solutions between artificial blood meals consisting of defibrinated sheep blood (Colorado Serum Company, Denver, CO) or bovine blood.

DENV2 (strain: New Guinea C (NGC), NCBI GenBank: AF038403) was propagated in C6/36 cells at a multiplicity of infection of 0.01 for 6 d using MEM supplemented with 10% FBS, 1% Pen/Strep, 1% L-Glutamine, and 1% nonessential amino acids. The supernatant from DENV2-infected cells was collected, clarified by centrifugation at 3,200 ×*g* for 10 min at 4° C in a swing bucket rotor, and aliquots were frozen at −80° C until use. Artificial infectious blood meals were

prepared by washing red blood cells from bovine with PBS followed by mixing with virus-infected cell culture medium to a titer of 5×10^6 pfu/mL (reaching 30% hematocrit) and supplementing the meal with 1 mM ATP. Using one glass feeder per carton, artificial meals were provided to mosquitoes for 30 min at 37° C. Fully engorged mosquitoes were selected for downstream experiments.

Purification of DENV2 for VOPBA. The supernatant from DENV2 (strain: NGC)-infected C6/36 cells (6 ml) was collected 6 d postinfection and clarified by centrifugation at 3,200 ×*g* for 60 min at 4° C using a swing bucket rotor. The clarified DENV2 suspension was then digested with bovine trypsin (Millipore Sigma, Saint Louis, MO) as previously described (16). In brief, the DENV2 culture was digested with PBS dialyzed 0.1 mg/ml bovine trypsin for 30 min at room temperature (RT). Trypsin was inactivated by the addition of PBS dialyzed STI (ThermoFisher Scientific, Waltham, MA) to a concentration of 8 mg/mL and incubated for another 30 min at RT before purification. The digested DENV2 culture was carefully layered over 3 mL of a 20% sucrose solution in a 13.2 mL thin wall polypropylene tube as previously described (38). The suspension was ultracentrifuged at 30,000 rpm (110,880 ×*g*) for 3 h at 4° C in a Beckman SW-41 Ti rotor. After centrifugation, the supernatant was carefully removed, and the tubes were inverted to air dry for 20 min at RT. Pellets were resuspended in 100 mM HEPES buffer pH 7.9, supplemented with 50 mM NaCl at 4° C and immediately centrifuged in an Eppendorf microcentrifuge at 16,000 ×*g* for 10 min at 4° C. The supernatant was removed, and the pellet was resuspended in 10 mM Tris-Cl pH 8.0, 120 mM NaCl. The purified DENV2 stocks were analyzed by the plaque assay and diluted to a final concentration of 1×10^6 PFU/ml before being used in downstream assays.

VOPBA. Mosquito midguts were dissected at 48 h postfeeding of mosquitoes on human serum. The midguts were cleaned with PBS and placed in solubilization buffer (15 mM Tris pH 8.0, 150 mM NaCl, 5 mM EDTA, and 1x cOmplete ULTRA protease inhibitor, Roche, San Francisco, CA). The midguts were homogenized with a motorized pestle before being frozen at -80° C to lyse the cells, thawed, and then homogenized a second time with a motorized pestle. The midgut lysates were centrifuged at 0.5 ×*g* at 4° C for 10 min before the supernatant was transferred to an ultracentrifuge tube and centrifuged at 100,000 ×*g* at 4° C for 20 min to produce

the cytosolic fraction. The supernatant (cytosolic fraction) was removed and stored at $-80°$ C. The pellet was resuspended in solubilization buffer supplemented with 0.5% Triton X-100 to a concentration of 0.25 mg/μL and centrifuged at 16,000 $×g$ at 4° C for 15 min. The supernatant (soluble membrane fraction) was saved and stored at $-80°$ C. The final pellet was resuspended in solubilization buffer to a concentration of 0.5 mg/μL. Both, the cytosolic, soluble membrane, and insoluble membrane fractions were diluted with 4 × LDS sample buffer and boiled for 10 min before being electrophoretically separated on a 4-12% NuPAGE Bis-Tris gel (Invitrogen, Waltham, MA). Following gel electrophoresis, the separated proteins were transferred to a nitrocellulose membrane and the proteins were denatured and refolded on the membrane according to an adapted protocol (39). In brief, membranes were incubated with refolding buffer (100 mM NaCl, 20 mM Tris pH 7.6, 0.5 mM EDTA, 10% glycerol, 0.1% Tween-20, and 2% milk) for 30 min at RT with reducing concentrations of Guanidine-HCl ranging from 6 M, 3 M, 1 M, 0.01 M, and 0 M. The membranes were then blocked overnight in blocking solution (PBST with 5% milk). Membranes were washed with 4 × blocking buffer before incubation with 2 × 10^5 PFU of DENV2 in 1 mL of blocking buffer in a sealed bag for 2 h at RT. Membranes were again washed with 4 × blocking buffer before being incubated with a 1:1,000 dilution of orthoflavivirus-specific 4G2 monoclonal antibody (Millipore Sigma, Saint Louis, MO) in blocking buffer for 1 h at RT. Membranes were then incubated with anti-mouse HRP in a 1:7,000 dilution for 1 h at RT. Membranes were washed 2 × with blocking buffer and 2 × with TBST before being developed with SuperSignal™ West Dura HRP substrate (ThermoFisher Scientific). Membranes were imaged on the IBright 1,500 imaging system (Invitrogen, Waltham, MA).

2D gel analysis. For 2D far-western blots, the midgut protein isolates were prepared as described above. However, before electrophoresis protein isolates were diluted 2 × in DeStreak Rehydration solution (Cytiva, Marlborough, MA) containing 0.1 M DTT before separation at 4 to 9 pH using a Novex IEF gel system (ThermoFisher Scientific). After protein transfer to the nitrocellulose membrane, it was incubated with purified DENV2 as described above. The areas of detection were aligned with a Coomassie-stained 2D gel, and the corresponding bands were excised for mass spectrometry analysis.

Recombinant Proteins. The full-length coding sequences of AAEL011180 and AAEL017349 with signal peptides and stop codons removed were PCR amplified from a cDNA library derived from *Ae. aegypti* midgut tissue using cloneAmp HiFi PCR Mix (Takara Bio, San Jose, CA) with gene-specific primers Fwd 1/Rev 1 and Fwd 2/Rev 2 described in *SI Appendix*, Table S5. The pET17 plasmid vector (EMD Millipore, Saint Louis, MO) was linearized by digest with NdeI and XhoI (New England Biolabs, Ipswich, MA) before each similarly digested amplicon was inserted using In-Fusion Cloning (Takara Bio). Using the resulting recombinant plasmids, protein expression was induced in One Shot™ BL21 chemically competent *E. coli* (Invitrogen, Waltham, MA) with 1 mM isopropyl β-D-thiogalactopyranoside (IPTG) for 4 h at 37° C. Cell pellets were collected, and it was determined via Coomassie staining that HSC-70 was expressed in the soluble fraction, while EPrRec localized within inclusion bodies. HSC-70 pellets were extracted with B-PER™ complete bacterial protein extraction reagent (ThermoFisher Scientific) and supplemented with Benzonase (Millipore Sigma) at 25 U/mL. The solution was centrifuged at 30,000 $×g$ for 15 min at 4° C before being purified by nickel affinity chromatography and eluted in 50 mM Tris-HCl pH 7.5 1 M NaCl with 250 mM imidazole. A buffer exchange was performed using Amicon Ultra-15 centrifugal filter units with a 30 kDa MWCO to remove imidazole before storage in 50 mM Tris-HCl pH 7.5 (supplemented with 1 M NaCl) at $-20°$ C.

EPrRec cell pellets were resuspended in 20 mM Tris-HCl pH 8.0 and sonicated in 30 s increments. The pellets were collected and washed with Tris buffer containing 1% Triton X-100, before being washed 3 × with 20 mM Tris-HCl pH 8.0. Inclusion bodies were resuspended in Tris-HCl pH 8.0 supplemented with 6 M guanidine hydrochloride at RT for 30 min, then DTT was added to a concentration of 10 mM and incubated for 30 before centrifugation at 15,000 $×g$ for 10 min at 20° C to remove the pellet. The recombinant protein in the supernatant was refolded by dropwise dilution into a large volume of 50 mM CAPS buffer, pH 10.0 containing 0.5 M L-arginine, 1 mM EDTA, 0.5 mM GSSG, and 5 mM GSH. Following refolding, the solutions were stirred for 1 h before being stored overnight at 4° C. The protein was concentrated by tangential flow filtration followed by diafiltration and purified by size exclusion chromatography using an AKTA

purifier 10 system (Cytiva). The protein was then concentrated by nickel affinity chromatography, before being dialyzed and stored in Tris-HCl pH 8.0 (supplemented with 150 mM NaCl) at $-20°$ C.

Western Blot. Mosquito midguts from WT *Ae. aegypti* females were dissected in PBS and placed in solubilization buffer (15 mM Tris pH 8.0, 150 mM NaCl, 5 mM EDTA, and 1 × Complete Ultra Protease inhibitor). The midguts were homogenized with a mortar and pestle before being diluted with 4 × LDS sample buffer and boiled for 10 min. The proteins were electrophoretically separated on a 4 to 12% NuPAGE gel and transferred to a nitrocellulose membrane with an iBlot™ 2 Gel Transfer Device (ThermoFisher Scientific). The membranes were blocked overnight in blocking solution (PBST with 5% milk) at 4° C and washed 4 × with blocking buffer before incubation with primary antibody, rabbit IgG anti-P47Rec (AGAP006398), at a dilution of 1:5,000 in blocking buffer for 2 h at RT. Membranes were washed 4 × for 10 min with blocking buffer before incubation with secondary antibody anti-rabbit IgG-HRP at a dilution of 1:10,000 in blocking buffer for 1 h at RT. Membranes were washed 3 × with blocking buffer and 1 × with TBST before being developed with SuperSignal™ West Dura HRP substrate. Membranes were imaged on an IBright 1,500 imaging system. As a loading control, membranes were stripped with Restore™ Western Blot Stripping Buffer (ThermoFisher Scientific) for 10 min at 37° C. The membranes were then washed 4 × with TBST and blocked in TBST with 5% BSA for 3 h at RT. Membranes were washed 3 × in TBST with 5% BSA and incubated with anti-actin HRP at a dilution of 1:10,000 for 1 h at RT. Membranes were washed 3 × in TBST supplemented with 5% BSA and 1 × with TBST before being developed with SuperSignal™ West Dura HRP substrate. Membranes were imaged on an IBright 1,500 imaging system.

Immunofluorescence Assay. Mosquitoes were dissected in PBS (KD Medical, Columbia, MD) at 24 h postserum meal or 4 d post-DENV2 infection. If the midguts contained blood meal remnants, they were immediately placed in 4% paraformaldehyde fixative at RT for 45 s to partially fix the tissue and then placed into ice-cold PBS for 5 min. Using a dissection needle, midguts were opened lengthwise in PBS to remove the bolus. All midguts were fixed in 4% paraformaldehyde in PBS for 1 h at RT. After fixation, midguts were washed 2 × for 15 min with 0.1% Triton X-100 in PBS at RT, before permeabilizing and blocking the tissue for 1 h in PBST (1% BSA, 0.1% Triton X-100, 0.1% gelatin, in PBS pH 7.2) at RT. Midguts were then incubated overnight at 4° C with rabbit IgG anti-6398 (EPrRec) at 5 μg/mL, and monoclonal 4G2 orthoflavivirus-specific mouse IgG at 1:500 in PBST. The tissues were washed 3 × for 15 min in PBST prior to incubation with the secondary antibody, anti-rabbit Alexa-fluor 488 (ThermoFisher Scientific), or anti-mouse-Alexa-fluor 594 (ThermoFisher Scientific) at a 1:1,000 dilution in PBST for 3 h at RT. Midguts were washed 3 × for 15 min with PBST before staining with Alexa-fluor 647 phalloidin (ThermoFisher Scientific) at a 1:40 dilution in PBS, and nuclei were stained with a final concentration of 2 μM Hoechst (ThermoFisher Scientific) in PBS for 30 min. The tissues were mounted with Prolong gold (ThermoFisher Scientific) and analyzed by confocal microscopy. Images were captured with a Leica TCS SP8 confocal microscope (Leica Microsystems, Wetzlar, Germany) with a 63× oil immersion objective. Images were processed using Leica Application Suite X (Leica Microsystems, Wetzlar, Germany).

ELISA. The protein interactions between DENV2 NGC and the proteins encoded by AAEL011180 and AAEL017349 were examined in ELISAs. 96-well ELISA plates (Immunolon 96-well plates, ThermoFisher Scientific) were coated in duplicates with 100 μL of recombinant protein at a concentration of 5 μg/mL diluted in BupH™ carbonate-bicarbonate buffer (0.2 M carbonate-bicarbonate, pH 9.4) and maintained at 4° C overnight. Plates were then washed 10× with PBST and blocked with 5% BSA in PBST for 1 h at RT. Plates were then incubated for 1 h at RT with a dilution series of the corresponding recombinant protein starting at a concentration of 8 μg/mL down to 0.125 μg/mL, or with a dilution series of DENV2 starting at 1 × 10^7 PFU down to 1 × 10^3 PFU. Plates were washed 10× with PBST and were then incubated with 1 μg/mL anti-AAEL011180, anti-KDEL (ThermoFisher Scientific), or 4G2 monoclonal antibody (EMD Millipore) for 1 h at RT. After an additional 10 washes, the plates were incubated with 1:10,000 dilutions of anti-mouse IgG-HRP (ThermoFisher Scientific) or anti-rabbit IgG-HRP (ThermoFisher Scientific) for 1 h at 37° C. The plates were washed a final 10× and detection was performed using TMB Ultra (ThermoFisher Scientific). Following a 30-min incubation, an equal volume of stop solution (ThermoFisher

7 of 9

Scientific) was added, and the absorbance was measured at 450 nm with a versaMax microplate reader (VWR, Radnor, PA).

Surface Plasmon Resonance Assay. To determine the binding affinity of EPrRec to DENV2 E glycoprotein, a surface plasmon resonance assay was performed on a BIAcore T100 instrument. DENV2 E glycoprotein (AB cam, Waltham, MA) was diluted to 5 µg/mL in immobilization buffer (10 mM sodium acetate pH 5.0, Cytiva) and immobilized by amine coupling on the surface of a CM5 sensor chip until the target density of 1,600 RU was reached. A blank flow cell was used as a negative control channel. K_D values were determined by performing kinetic experiments with recombinant AAEL011180 as the analyte at concentrations ranging from 500 nM to 7.8125 nM. The analyte flowed for 200 s at 30 mL/min in HBS-P buffer (10 mM HEPES, 150 mM NaCl, 0.005% surfactant P20, pH 7.4, Cytiva). Dissociation was measured for 600 sec, and the active cell was regenerated with 45 s pulse of 10 mM HCl at 40 µL/min between runs. Biacore T100 Evaluation software 2.0.4 was used for kinetic evaluation.

dsRNA-Mediated Gene Silencing. Individual female mosquitoes were injected intrathoracically with 180 nl of 6 µg/µL dsRNA solution 1 d postemersion. The control LacZ dsRNA was produced as previously described (40). The AAEL011180 and AAEL017349 dsRNA templates were designed using E-RNAi software to ensure off-target effects were minimized and amplified from cDNA templates obtained from midgut tissue using gene-specific primers Fwd 3/Rev 3 and Fwd 4/Rev 4 (*SI Appendix*, Table S5). dsRNA was generated using a MEGAscript™ T7 transcription kit (Invitrogen). Gene silencing was assessed 4 d postinjection in sugar-fed and blood-fed mosquitoes with RT-qPCR using the DyNAmo HS SYBR Green qPCR Kit (ThermoFisher Scientific) and primers Fwd 5/Rev 5, Fwd 6/Rev 6, and Fwd 7/Rev 7 (*SI Appendix*, Table). Relative quantification results were normalized against the *Ae. aegypti* ribosomal protein s7 ribosomal gene (RPS7) as an internal standard and analyzed with the $^{\Delta\Delta}CT$ method. Statistical differences in relative fold-change values between conditions were analyzed using a *t* test (GraphPad, vs. 9). Each experiment was performed on 3 biological replicates using 15 midguts per replicate per condition, and qPCR was performed in triplicates (technical replicates) for each sample.

Establishment of a Hemizygous ΔEPrRec Knock-Out Line of *Ae. aegypti*. A fluorescent eye marker was inserted into the 5′ end of Exon II (at nucleotide position 80 of the coding sequence) of AAEL011180 in *Ae. aegypti* (strain LVP) using CRISPR/Cas9 mediated genome editing. Three potential sgRNAs (1, 2, 3; *SI Appendix*, Table S5) targeting the 5′ end of the open reading frame of AAEL011180 exon II were identified using CHOPCHOP (41–43) and initially tested in a transient assay for genomic DNA cleavage activity using preblastoderm embryos of *Ae. aegypti*. Embryos were collected from hypergravid females over a 15-min period then manually aligned, transferred to double-face Scotch tape (Scotch Brand, St. Paul, MN), and covered with Halocarbon 27 oil (Millipore Sigma). Preblastoderm embryos were then injected no later than 30 min after collection using a Femtojet microinjector (Eppendorf, Hamburg, Germany) set to a constant injection pressure of 600 hPa and a backpressure of 250 hPa. The halocarbon 27 oil was immediately washed from the embryos with deionized water and the embryos were allowed to develop for 16 to 24 h in a humid Petri dish prior to genomic DNA extraction using DNAzol (ThermoFisher Scientific). Three sets (1 set per sgRNA) of ~100 preblastoderm *Ae. aegypti* embryos were microinjected with a mix containing 300 ng/µL Cas9-NLS protein (PNABio, Thousand Oaks, CA) complexed individually with 80 ng/µL sgRNAs (#1, #2, or #3) synthesized using the ENGen sgRNA kit (New England Biolabs). To confirm sgRNA cleavage activity, the genomic locus surrounding Exon II of AAEL011180 was then amplified through PCR using GOTaq (Promega, Madison, WI) under the following cycling conditions: 95° C 5 min, followed by 35 cycles of 95° C for 15 sec, 60° C for 20 sec, 72° C for 90 sec, followed by a final extension of 5 min at 72° C using primers Fwd 9/Rev 10 (*SI Appendix*, Table S5). PCR products were gel purified using the gel extraction kit from Zymo Research (Irvine, CA), sequenced at the University of Missouri Genomics Technology Core (Columbia, MO), and assessed for trace decay at the predicted CRISPR/Cas9 target sites. Eventually, one active sgRNA (#3) was selected and a donor plasmid was constructed around the target site of sgRNA #3 using the pBluescript KS+ plasmid vector (44). The donor plasmid consisted of an eye marker expression cassette (mCherry under the control of the 3 × P3 promoter and the SV40 large T antigen polyadenylation terminator (45, 46) flanked by 400 bp homology arms. The upstream homology arm was directionally cloned into pBluescript using PspOMI/XhoI, followed by the downstream homology arm using XbaI/SacII. The attP-3 × P3-mCherry-SV40 cassette was then amplified from an existing plasmid, digested with XhoI, and cloned into the homology arm destination vector using XhoI and screened for directionality. Primers used to construct the donor plasmid (Fwd 11/Rev 11, Fwd 12/Rev 12, Fwd 13/Rev 13) are described in *SI Appendix*, Table S5.

Following identification of an active sgRNA and the construction of the corresponding donor plasmid, an injection mix was set up that contained: 200 ng/µL Cas9-NLS (PNABio), 80 ng/µL sgRNA, 100 ng/µL ku70 dsRNA to suppress NHEJ activity (47), and 135 fmol/µL donor plasmid. Preblastoderm *Ae. aegypti* embryos were injected and surviving founders were individually outcrossed to parental LVP *Ae. aegypti* mosquitoes. Outcrossed G_0 founders were then provided three blood meals (defibrinated sheep blood, Colorado Serum, Denver, CO), and allowed to lay the eggs representing the G_1. Following hatching, G_1 individuals were screened for the presence of mCherry expressing eyes and those selected individuals were outcrossed a second time to the recipient strain to obtain six lines of mosquitoes in which AAEL011180 was disrupted.

Confirmation of Transgene Insertion by PCR and Sequencing. To confirm site-specific insertion of the transgene, genomic DNA was extracted from individual ΔEPrRec mosquitoes using phenol/chloroform. Primer pairs annealing to genomic DNA surrounding the expected 5′ (Fwd 9/Rev 9) and 3′ (Fwd 8/Rev 8) donor insertion sites are described in *SI Appendix*, Table S5. PCRs were conducted using Platinum SuperFi DNA polymerase (ThermoFisher Scientific). Resulting PCR products were separated by gel electrophoresis, and individual bands were excised and purified with the Zymoclean Gel DNA Recovery Kit (Zymo Research) and sent for Sanger Sequencing (Eurofins Genomics, Louisville, KY) to confirm the correct donor insertion for targeted gene disruption. Genotyping was performed on individual mosquitoes to identify heterozygous and homozygous individuals. A multiplex PCR was established with one forward primer (Fwd 10, annealing to a DNA sequence outside the donor insertion site) and two reverse primers (*SI Appendix*, Table S5). One of the reverse primers (Rev 9) was specific to the inserted donor yielding a PCR product of 375 bp (ΔEPrRec allele) in combination with the forward primer. The second reverse primer (Rev 10) was specific to the *EPrRec* gene to yield a PCR product of 130 bp (WT allele) in combination with the forward primer. One mosquito leg from each mosquito was placed into 10 µL of nuclease-free H_2O and heated on a thermocycler at 98° C for 10 min to release the genomic template DNA. Dreamtaq HotStart PCR master mix (ThermoFisher Scientific) was used to amplify the genomic DNA under the following cycling conditions: 98° C 3 min, followed by 35 cycles of 95° C for 30 sec, 54° C for 30 sec, 72° C for 60 sec, followed by a final extension at 72° C for 5 min. Following amplification, the DNA amplicons were separated by gel electrophoresis in a 1% agarose gel and visualized on an iBright 1,500 gel imager (Invitrogen) to assess the genotype.

Plaque Assay. Plaque assays were performed to determine DENV2 titers in individual midguts. Midguts were dissected in PBS at 5 or 7 d postinfection and homogenized in 200 µL of DMEM (2% FBS and 1% Pen/Strep) using sterile glass beads in a Bullet Blender (Next Advance Inc., Troy, NY). Serial dilutions (10×) were prepared and plated in 24-well plates seeded with BHK 21 cells. Each well of confluent cells was infected with 100 µL of sample for 1 h before 1 mL of an overlay consisting of DMEM (2% FBS and 2% Pen/Strep) with 0.8% methylcellulose (Sigma) was added. The plates were incubated for 5 d at 37° C under 5% CO_2 supplementation. Thereafter, the overlays were removed and cells were stained with 1% crystal violet solution before plaques were counted and recorded as PFU/mosquito.

Data, Materials, and Software Availability. All study data are included in the article and/or *SI Appendix*.

Author affiliations: aLaboratory of Malaria and Vector Research, National Institutes of Allergy and Infectious Diseases, NIH, Rockville, MD 20852; and bDepartment of Veterinary Pathobiology, University of Missouri, Columbia, MO 65211

1. M. G. Guzman, E. Harris, Dengue. *Lancet* **385**, 453–465 (2015).
2. T. P. Monath, Dengue: The risk to developed and developing countries. *Proc. Natl. Acad. Sci. U.S.A.* **91**, 2395–2400 (1994).
3. P. A. H. Organization, *Epidemiological Update Increase in Dengue Cases in The Region of The Americas*, (PAHO, 2024) pp. 1-14.
4. S. Bhatt *et al.*, The global distribution and burden of dengue. *Nature* **496**, 504–507 (2013).
5. O. J. Brady *et al.*, Refining the global spatial limits of dengue virus transmission by evidence-based consensus. *PLoS Negl. Trop. Dis.* **6**, e1760 (2012).
6. A. W. Franz *et al.*, Tissue barriers to arbovirus infection in mosquitoes. *Viruses* **7**, 3741–3767 (2015).
7. M. I. Salazar *et al.*, Dengue virus type 2: Replication and tropisms in orally infected Aedes aegypti mosquitoes. *BMC Microbiol.* **7**, 9 (2007).
8. D. M. Watts *et al.*, Effect of temperature on the vector efficiency of Aedes aegypti for dengue 2 virus. *Am. J. Trop. Med. Hyg.* **36**, 143–152 (1987).
9. Y. S. Hahn *et al.*, Nucleotide sequence of dengue 2 RNA and comparison of the encoded proteins with those of other flaviviruses. *Virology* **162**, 167–180 (1988).
10. S. Mukhopadhyay, R. J. Kuhn, M. G. Rossmann, A structural perspective of the flavivirus life cycle. *Nat. Rev. Microbiol.* **3**, 13–22 (2005).
11. R. J. Kuhn *et al.*, Structure of dengue virus: Implications for flavivirus organization, maturation, and fusion. *Cell* **108**, 717–725 (2002).
12. W. Zhang *et al.*, Visualization of membrane protein domains by cryo-electron microscopy of dengue virus. *Nat. Struct. Mol. Biol.* **10**, 907–912 (2003).
13. W. D. Crill, J. T. Roehrig, Monoclonal antibodies that bind to domain III of dengue virus E glycoprotein are the most efficient blockers of virus adsorption to Vero cells. *J. Virol.* **75**, 7769–7773 (2001).
14. L. Dai *et al.*, Structures of the Zika virus envelope protein and its complex with a flavivirus broadly protective antibody. *Cell Host Microbe* **19**, 696–704 (2016).
15. Y. Chen, T. Maguire, R. M. Marks, Demonstration of binding of dengue virus envelope protein to target cells. *J. Virol.* **70**, 8765–8772 (1996).
16. A. Molina-Cruz *et al.*, Effect of mosquito midgut trypsin activity on dengue-2 virus infection and dissemination in Aedes aegypti. *Am. J. Trop. Med. Hyg.* **72**, 631–637 (2005).
17. S. L. Allison *et al.*, Mutational evidence for an internal fusion peptide in flavivirus envelope protein E. *J. Virol.* **75**, 4268–4275 (2001).
18. D. E. Klein, J. L. Choi, S. C. Harrison, Structure of a dengue virus envelope protein late-stage fusion intermediate. *J. Virol.* **87**, 2287–2293 (2013).
19. Y. Modis *et al.*, Structure of the dengue virus envelope protein after membrane fusion. *Nature* **427**, 313–319 (2004).
20. P. Sakoonwatanyoo, V. Boonsanay, D. R. Smith, Growth and production of the dengue virus in C6/36 cells and identification of a laminin-binding protein as a candidate serotype 3 and 4 receptor protein. *Intervirology* **49**, 161–172 (2006).
21. J. Reyes-del Valle, R. M. del Angel, Isolation of putative dengue virus receptor molecules by affinity chromatography using a recombinant E protein ligand. *J. Virol. Methods* **116**, 95–102 (2004).
22. M. L. Muñoz *et al.*, Proteomic identification of dengue virus binding proteins in Aedes aegypti mosquitoes and Aedes albopictus cells. *Biomed. Res. Int.* **2013**, 875958 (2013).
23. A. Kuadkitkan *et al.*, Identification and characterization of prohibitin as a receptor protein mediating DENV-2 entry into insect cells. *Virology* **406**, 149–161 (2010).
24. V. M. Cao-Lormeau, Dengue viruses binding proteins from Aedes aegypti and Aedes polynesiensis salivary glands. *Virol. J.* **6**, 35 (2009).
25. K. I. Hidari, T. Suzuki, Dengue virus receptor. *Trop. Med. Health* **39**, 37–43 (2011).
26. A. Molina-Cruz *et al.*, Plasmodium falciparum evades immunity of anopheline mosquitoes by interacting with a Pfs47 midgut receptor. *Proc. Natl. Acad. Sci. U.S.A.* **117**, 2597–2605 (2020).
27. L. H. Figueiredo Prates *et al.*, Challenges of robust RNAi-mediated gene silencing in Aedes mosquitoes. *Int. J. Mol. Sci.* **25**, 5218 (2024).
28. E. S. T. L. Alves *et al.*, The heat shock protein Hsc70-3 mediates an anti-apoptotic response critical for Plasmodium evasion of Anopheles gambiae immunity. *Microbiol. Spectr.* **11**, e0094023 (2023).
29. H. Y. Chee, S. AbuBakar, Identification of a 48kDa tubulin or tubulin-like C6/36 mosquito cells protein that binds dengue virus 2 using mass spectrometry. *Biochem. Biophys. Res. Commun.* **320**, 11–17 (2004).
30. J. Salas-Benito *et al.*, Evidence that the 45-kD glycoprotein, part of a putative dengue virus receptor complex in the mosquito cell line C6/36, is a heat-shock related protein. *Am. J. Trop. Med. Hyg.* **77**, 283–290 (2007).
31. C. Cruz-Oliveira *et al.*, Receptors and routes of dengue virus entry into the host cells. *FEMS Microbiol. Rev.* **39**, 155–170 (2015).
32. J. Rodrigues *et al.*, An epithelial serine protease, AgESP, is required for Plasmodium invasion in the mosquito Anopheles gambiae. *PLoS One* **7**, e35210 (2012).
33. C. P. Ponting *et al.*, Novel protein domains and repeats in Drosophila melanogaster: Insights into structure, function, and evolution. *Genome Res.* **11**, 1996–2008 (2001).
34. S. Jiang *et al.*, DM9 domain containing protein functions as a pattern recognition receptor with broad microbial recognition spectrum. *Front. Immunol.* **8**, 1607 (2017).
35. C. B. Ocampo *et al.*, Differential expression of apoptosis related genes in selected strains of Aedes aegypti with different susceptibilities to dengue virus. *PLoS One* **8**, e61187 (2013).
36. M. Jäättelä *et al.*, Hsp70 exerts its anti-apoptotic function downstream of caspase-3-like proteases. *EMBO J.* **17**, 6124–6134 (1998).
37. C. T. Yeh *et al.*, The chaperone BiP promotes dengue virus replication and mosquito vitellogenesis in Aedes aegypti. *Insect Biochem. Mol. Biol.* **155**, 103930 (2023).
38. S. M. Jensen, C. T. Nguyen, J. C. Jewett, A gradient-free method for the purification of infective dengue virus for protein-level investigations. *J. Virol. Methods* **235**, 125–130 (2016).
39. Y. Wu, Q. Li, X.-Z. Chen, Detecting protein–protein interactions by far western blotting. *Nat. Protoc.* **2**, 3278–3284 (2007).
40. A. Molina-Cruz *et al.*, Reactive oxygen species modulate Anopheles gambiae immunity against bacteria and Plasmodium. *J. Biol. Chem.* **283**, 3217–3223 (2008).
41. K. Labun *et al.*, CHOPCHOP v2: A web tool for the next generation of CRISPR genome engineering. *Nucleic Acids Res.* **44**, W272–W276 (2016).
42. K. Labun *et al.*, CHOPCHOP v3: Expanding the CRISPR web toolbox beyond genome editing. *Nucleic Acids Res.* **47**, W171–W174 (2019).
43. T. G. Montague *et al.*, CHOPCHOP: A CRISPR/Cas9 and TALEN web tool for genome editing. *Nucleic Acids Res.* **42**, W401–W407 (2012).
44. M. A. Alting-Mees, J. M. Short, pBluescript II: Gene mapping vectors. *Nucleic Acids Res.* **17**, 9494 (1989).
45. C. Horn, B. Jaunich, E. A. Wimmer, Highly sensitive, fluorescent transformation marker for Drosophila transgenesis. *Dev. Genes Evol.* **210**, 623–629 (2000).
46. Y. Cui *et al.*, Cytoskeleton-associated gelsolin responds to the midgut distention process in saline meal-fed Aedes aegypti and affects arbovirus dissemination from the midgut. *FASEB J.* **38**, e23764 (2024).
47. S. Basu *et al.*, Silencing of end-joining repair for efficient site-specific gene insertion after TALEN/CRISPR mutagenesis in Aedes aegypti. *Proc. Natl. Acad. Sci. U.S.A.* **112**, 4038–4043 (2015).